

Journal of Design Against Fatigue
https://minerva-aset.com/JDAF

MINERVA ASET ISSN 2976-940X

Heat Treatment of 440C Stainless Steel: Mechanical and Electrochemical Behaviour

N. Chavda[1,2], A. Zomorodian[1*], A.H. Mahmoudi[2*]

[1] *Renishaw PLC, Wotton-Under-Edge, GL12 8JR, UK,*

[2] *School of Engineering, University of West of England, Frenchay Campus, Bristol BS16 1QY, UK,*

P A P E R I N F O

Paper history:
Received 8 September 2025
Received in revised form 3 November 2025
Accepted 5 November 2025

Keywords:
440C stainless steel; heat treatment; cryogenic processing; hardness; wear resistance; corrosion behaviour; martensitic transformation; microstructure; tribology

A B S T R A C T

Abstract This study aims to evaluate the effects of different heat treatment routes on the microstructure, mechanical properties, corrosion resistance, and tribological performance of 440C stainless steel, with comparative analysis against 416 martensitic stainless steel. Scanning electron microscopy (SEM) was employed to examine microstructural changes, while hardness was measured using standard tests. Corrosion behaviour was assessed through potentiodynamic polarization and open circuit potential (OCP) measurements, tribological performance via pin-on-disk tests, and mechanical properties using plastometry. Three heat treatment routes were investigated: double air tempering at 180°C after austenitising and air quenching, double vacuum tempering at 180°C, and nitrogen tempering at 180°C followed by cryogenic quenching and subsequent nitrogen tempering. Results indicate that all heat treatments significantly improve the mechanical properties of 440C stainless steel compared to untreated and heat-treated 416 stainless steel. Cryogenic treatment notably enhances both hardness and corrosion resistance more effectively than other methods, although its tribological performance under higher loads (15N) is inferior. These findings underscore the importance of tailoring heat treatment strategies to optimize 440C stainless steel for applications requiring high mechanical strength and corrosion resistance.

https://doi.org/10.62676/jdaf.2025.3.2.20

1. INTRODUCTION

Stainless steels have long been recognized for their corrosion resistance, mechanical strength, and versatility across industrial applications. Among them, 440C stainless steel, a high-carbon martensitic grade, stands out due to its exceptional hardness, wear resistance, and capacity for heat treatment. The development of stainless steels began in the early 20th century, with Harry Brearley's landmark discovery in 1913 of a chromium-rich steel alloy that resisted staining and corrosion[1]. This innovation laid the foundation for the stainless steel family, which has since evolved to include specialized grades tailored for specific performance requirements.

440C stainless steel emerged in the 1920s as a high-performance alloy within the martensitic category, characterized by a chromium content of approximately 16–18% and a carbon content ranging from 0.95–1.20%.[2] Its ability to undergo heat treatment enables the formation of a martensitic microstructure, which imparts high strength and hardness. These properties make 440C particularly suitable for applications requiring superior wear resistance and dimensional stability, such as precision bearings, surgical instruments, valve components, and cutting tools[3].

*Corresponding Author Email: Amir.Mahmoudi@uwe.ac.uk, a.h.mahmoudi@gmail.com, (Amir H. Mahmoudi), Amir.Zomorodian@Renishaw.com, (Amir Zomorodian)

Cite this article as: N. Chavda, A. Zomorodian, A.H. Mahmoudi, Heat Treatment of 440C Stainless Steel: Mechanical and Electrochemical Behaviour, ***Journal of Design Against Fatigue,*** Vol. 3, No. 2, (2025) 18-27, https://doi.org/10.62676/jdaf.2025.3.2.20



Copyright: © 2025 by the author(s). Published by Minerva ASET, Devon, UK. This is an open access article distributed under the terms and conditions of the Creative Commons Attribution (CC BY) License. (https://creativecommons.org/licenses/by/4.0/).

The mechanical properties of 440C stainless steel are central to its industrial utility. Its tensile strength typically ranges from 1,770 to 2,170 MPa [4], and when properly heat treated, it achieves hardness values between 58–62 HRC on the Rockwell scale. The high carbon content contributes to the formation of chromium carbides during heat treatment, which enhance wear resistance and impede dislocation motion, thereby improving durability and strength[5]. The microstructure of 440C primarily consists of martensite with retained austenite, and the balance between these phases can be manipulated through heat treatment to optimize toughness and impact resistance [3].

The grain size and distribution of carbides play a critical role in determining the alloy's mechanical and tribological performance. Finer grain structures, achieved through controlled cooling rates, improve toughness, while the presence of chromium carbides enhances wear resistance and edge retention[3, 6]. The transformation from austenite to martensite is essential for achieving high hardness, but conventional heat treatment often leaves retained austenite due to sub-zero martensite finish temperatures in high-carbon steels. This retained austenite can compromise dimensional stability and reduce hardness, particularly in applications involving cyclic loading or thermal fluctuations.

To address these limitations, cryogenic treatment has been introduced as an extension of conventional heat treatment. Cryogenic processing involves cooling the steel to temperatures as low as −196°C, typically using liquid nitrogen, to promote complete transformation of retained austenite into martensite. This process not only enhances hardness and wear resistance but also improves dimensional stability and reduces residual stresses [7]. Shallow cryogenic treatment (SCT) involves cooling to −80°C for several hours, while deep cryogenic treatment (DCT) extends the cooling to −196°C, often with controlled ramp-down rates to avoid thermal shock. Both methods have demonstrated improvements in mechanical performance, though the extent of enhancement depends on the alloy composition and prior heat treatment history.

The precipitation of carbides during cryogenic treatment further contributes to the strengthening mechanism. These carbides act as hard particles that resist abrasive wear and impede dislocation movement, thereby enhancing the alloy's durability in demanding environments. The body-centered tetragonal (BCT) lattice structure of martensite, formed during quenching, is responsible for the high hardness and strength of 440C stainless steel [8] [9]. The interaction between chromium and carbon during heat treatment leads to the formation of chromium carbides, which are uniformly distributed throughout the microstructure and play a vital role in wear resistance and edge retention. Carbon and carbide phases not only enhance the strength of steel but also play a crucial role in controlling its microstructure. They serve as nucleation sites and inhibit the growth of austenite grains. According to the phase diagram of 440C stainless steel, M7C3 and M23C6 carbides precipitate across a wide temperature range, making it challenging to achieve a full solution treatment where all carbides dissolve into the austenitic phase. Therefore, a partial solution treatment within the austenite-carbide region is recommended as an alternative. This approach effectively refines the austenite grain structure and improves the steel's mechanical properties. However, The resulting microstructure and mechanical performance of 440C steel are highly sensitive to the temperature and duration of the treatment[10]. Despite its advantages, the optimization of heat treatment routes for 440C stainless steel remains an active area of research. Various studies have explored the influence of tempering conditions, quenching media, and cryogenic protocols on the alloy's mechanical and electrochemical properties. For instance, it was [11] demonstrated that controlled tempering following cryogenic treatment can significantly enhance impact resistance without compromising hardness. Similarly, [12] highlighted the trade-offs between carbide formation and toughness, emphasizing the need for precise control over heat treatment parameters.

In light of these findings, the present study investigates the influence of three distinct heat treatment methods; double air tempering, double vacuum tempering, and nitrogen tempering with cryogenic quenching; on the microstructure, mechanical properties, corrosion behaviour, and tribological performance of 440C stainless steel. By comparing these treatments with heat-treated 416 stainless steel, the study aims to identify a process that maximizes mechanical performance while preserving electrochemical integrity. The goal is to develop a heat treatment strategy that enhances the alloy's suitability for applications requiring both high strength and corrosion resistance, thereby contributing to the broader understanding of martensitic stainless-steel optimization.

2. MATERIALS AND METHODS

In this study, two grades of martensitic stainless steel, 440C and 416 with standard chemical composition shown in the Table 1, were subjected to various heat treatment protocols to investigate their influence on microstructure, mechanical properties, corrosion resistance, and tribological behaviour. The materials were processed under controlled conditions to ensure consistency and reproducibility across all test groups.

Table 1: Chemical composition of the stainless steel, used in this study, according to the standard

Steel grade	C %	Cr %	S %	Fe%
S.S 440C	0.95-1.2	16-18	0-0.03%	base
S-S 416	0- 0.15	12-14	0.15-0.35	base

2.1 Test Groups

Several test groups were used in this study.

440C Annealed (440C AN)

The 440C stainless steel was annealed by heating to 850°C, held for 6 hours, and then cooled slowly to room temperature within the furnace. This treatment was designed to relieve internal stresses and homogenize the microstructure prior to further processing.

416 Heat Treated (416 HT)

The 416 stainless steel underwent a multi-stage heat treatment in a vacuum furnace. The temperature was first raised to 800°C and held for 5 minutes, followed by an increase to 1020°C, maintained for 15 minutes. The steel was then cooled to 1000°C, followed by quenching in nitrogen gas to achieve a hardened martensitic structure.

440C Group 1 (G1)

Samples were austenitized at 1040°C for 2 hours, followed by air quenching. The steel was then tempered in air at 180°C, quenched again in air and subjected to a second air tempering at 180°C. This route represents a conventional double tempering process in ambient atmosphere.

440C Group 2 (G2)

Similar to G1, the steel was austenitized at 1040°C for 2 hours and air quenched. However, tempering was conducted in a vacuum environment at 180°C, followed by air quenching and a second vacuum tempering at 180°C. This method aims to reduce oxidation and improve surface integrity during tempering.

440C Group 3 (G3)

This group underwent austenitization at 1040°C for 2 hours, followed by air quenching. The first tempering was performed using nitrogen gas at 180°C, followed by cryogenic quenching in liquid nitrogen at −100°C, and a final nitrogen gas tempering at 180°C. This route incorporates cryogenic treatment to transform retained austenite and enhance hardness and dimensional stability.

2.2 Hardness Testing

Hardness testing conducted using the Rockwell HRC hardness testing method using a Innovatest hardness tester, this applies 150 Kgf using a diamond shaped indenter with a dwell time of 4 second on the sample. To ensure that the hardness testing on all samples is both representative and comparable, the surfaces of the samples were ground to P1200. This preparation allowed the force to be applied evenly across the impact region. All five samples were indented ten times using the same indentation pattern this allowed for an average value across the sample and eliminating anomalous results caused by impurities or voids in the material. The Resistance to the applied load from the sample is calculated by using $HR = N - \frac{d}{D}$ where:

HR: Rockwell hardness value.
N: Total load applied to the indenter (kgf).
d: Depth of penetration of the indenter (mm).
D: Diameter of the indenter (mm)

A total of 10 indents were carried out on each sample. Data gathered is used to plot a comparative graph.

2.3 Plastometry

Plastometry is a relatively new method in used to gather data like yield stress, elastic modulus and ultimate tensile strength using a Brinell indenter and a profilometer to map the topography of the indent made on the material [13]. This method is a much faster and less preparation needed for getting data in comparison to traditional tensile testing. Although due to the process still being standardised, it is not a thoroughly proven method accepted by all industries. Plastometry testing, using Plastometrex Indentation Plastomer, requires a smooth sample surface so the samples polished with sand pater grade P1200. The samples placed under a spherical indenter which applies a 3500 kN load to the samples to achieve a indentation depth of 110µm. The software carries out an iterative finite element method (FEM) simulation of the test until the best fit set of true stress/strain. A profilometer is used to measure the profile of the indent in order to use this data to calculate load and displacement.

2.4 Tribology and Pin-on-Disc Test

Friction wear testing conducted on TBR3 Tribometer with the sample material being tested against a diamond surface (Figure 1). All samples finished using Electrical Discharge Machining (EDM) to create the same surface finish across all samples. A 6mm diamond ball placed on the surface of the EDM'd samples with an applied load of 5N,10N & 15N in three separate tests per sample. The sample spins at 150 cm/s for a total of 30k cycles per load. The wear track is analysed using an optical profiler to determine the volume of material removed from the surface.



Figure 1 – Anton Paar TBR3 Tribometer

2.5 Etching

Sample preparation for etching consisted of samples ground to p400 grit followed by incrementally polishing the samples to a mirror surface finish using 9µ and 3µ polycrystalline diamond suspension on rotating polishing pads. 0.02µ colloidal Silica suspension is used as the final step of the polishing process to achieve the desired surface finish. The samples are etched using Viella's reagent with 416 & 440C AN etched for 60 seconds and G1-G3 etched for 30 seconds. The etched samples are then imaged on a Keyence microscope (Figure 5) at 1000x magnification.

2.6 EBSD

Electron Backscatter Diffraction (EBSD) is a technique used in a Scanning Electron Microscope (SEM) to analyse the crystallographic structure of materials. It involves directing an electron beam at a tilted sample, causing electrons to diffract and form a diffraction pattern. This pattern reveals information about the crystal orientation and phase of the material, making EBSD invaluable for studying the microstructure of crystalline materials. To prepare the samples for EBSD a mirror surface finish is required therefore the same polishing steps as for etching are required. An additional step is used to remove any surface imperfections on the sample where a Buehler Vibromet is used for 2 hours on the samples. The sample is mounted to a SEM fixturing at 70 degrees for analysis. Electrons are fired at the surface of the sample are backscattered and the diffraction patterns are detected to identify grain orientation.

2.7 Microstructural analysis

Analysis of the microstructure provides critical insights into the properties and behaviour of materials by revealing details such as grain size, phase distribution, and the presence of defects like dislocations and voids. Scanning Electron Microscopy (SEM) uses a focused beam of electrons to scan the surface of a specimen, producing high-resolution images that reveal detailed surface topography and composition. The interaction of the electron beam with the sample generates various signals, including secondary electrons (SE) and backscattered electrons (BSE), which are used to form images and provide information about the sample's surface and near-surface structure and composition. Images are taken at 1000x, 1500x & 5000x using backscatter and at 1000x using secondary electrons. For detailed chemical analysis Energy Dispersive X-ray Spectroscopy (EDS) is carried out at 1500x magnification on BED-C on regions of interest to identify the elements present. The grain size distribution was calculated using the Heyn Intercept Method [14] using randomized lines to use the line length over the count the number of grain boundary intersections to give an average grain size value

2.8 Corrosion Testing

Corrosion testing is carried out using a three-electrode cell setup. The working electrode (WE) is the sample material (440C), the reference electrode (RE) is Silver/Silver Chloride (Ag/AgCl), and the counter electrode (CE) is graphite. The test solution is prepared with a concentration of 0.1M NaCl. Initially, the open circuit potential (OCP) of the working electrode is measured for at least 30 minutes to ensure stability. Following the OCP measurement, a Potentiodynamic polarisation test is performed in a 0.1M chloride solution. The potential is swept from 0.3V below the OCP to 0.6V above the OCP. During this sweep, the current density and potential is recorded. The data obtained from the Potentiodynamic polarisation test is used to create a Tafel plot, which facilitated the determination of corrosion current density, corrosion potential, and passivation behaviour.

3. RESULTS & DISCUSSION

3.1 Hardness testing

The results of the hardness, reported in Table 2, represent the average of ten repeated tests per sample. The standard deviation was found to be low and therefore was not reported separately in the table. The data show that the hardness of 440C AN is significantly lower than that of 416 HT. The effect of heat treatment on 440C is clearly reflected in the hardness values, which exceed those of 416 HT by approximately 15 HRC. Among the heat-treated 440C samples, hardness values are consistent, with sample G3 exhibiting the highest hardness.

Table 2 – Hardness Testing

Sample	*416 HT*	*440C AN*	*G1*	*G2*	*G3*
Average Hardness (HRC)	43.2	18.9	58.4	57.5	59.2

Prior to heat treatment, 440C stainless steel primarily consists of a soft, annealed microstructure dominated by ferrite and retained austenite, with minimal martensitic content. This phase configuration results in relatively low hardness and limited wear resistance. Upon undergoing heat treatment, particularly austenitization followed by quenching, the microstructure transforms significantly, with the formation of martensite as the dominant phase[15]. The degree of hardness enhancement depends on the specific heat treatment route employed. Conventional air quenching followed by tempering leads to moderate hardness due to partial martensitic transformation and carbide precipitation. Vacuum tempering improves surface integrity and hardness slightly further. In contrast, cryogenic treatment promotes a more complete transformation of retained austenite into martensite and enhances carbide dispersion, resulting in significantly higher hardness[16]. The superior mechanical performance observed in cryogenically treated 440C stainless steel is attributed to the fully martensitic matrix, which is the primary source of increased hardness. The finely distributed chromium carbides further enhance wear resistance and microstructural stability.

3.2 Microstructure

Sample etching revealed the microstructure of the samples leaving the grain boundaries and phases visibly identifiable (Figure 2) by use of optical microscopy (not shown here) and using the SEM. Precipitates have been observed throughout the 440C heat treated samples. These precipitates can be found scattered across the whole grain with larger ones typically seen on grain boundaries. Grain boundaries are more prominent on 440C heat treated samples with 416 HT showing a needle like structure which is the martensite phase within the material. Martensite plays a significant role in the hardness of a material, its hardness is primarily due to the quenching of austenite, which traps carbon atoms within the crystal structure, creating a highly strained body centered tetragonal form. This process results in a large number of dislocations, which significantly increase the hardness of the material. Energy-dispersive X-ray spectroscopy (EDS) analysis, as shown in Figure 3, reveals that the precipitate regions in heat-treated AISI 440C stainless steel contain elevated levels of chromium and carbon, strongly suggesting the formation of chromium carbides. This finding is consistent with previous studies on the microstructural evolution of 440C, where austenite serves as the matrix phase and is typically accompanied by two dominant carbide types: $M_{23}C_6$ and M_7C_3 [17, 18]. The EDS data further indicate compositional differences between the darker and lighter regions of the precipitates. The darker areas exhibit a higher chromium concentration and are therefore most likely associated with $M_{23}C_6$ carbides, while the lighter regions, with lower chromium content, correspond to M_7C_3 carbides. These phase distinctions are clearly observable under scanning electron microscopy (SEM), which highlights the contrast in morphology and elemental distribution. EDS on 416 HT(not shown here) revealed the dark spots are Manganese Sulphate precipitate, this allows for easier machinability of the metal but reduces the metals corrosion resistance and can be used as crack propagation sites[19].

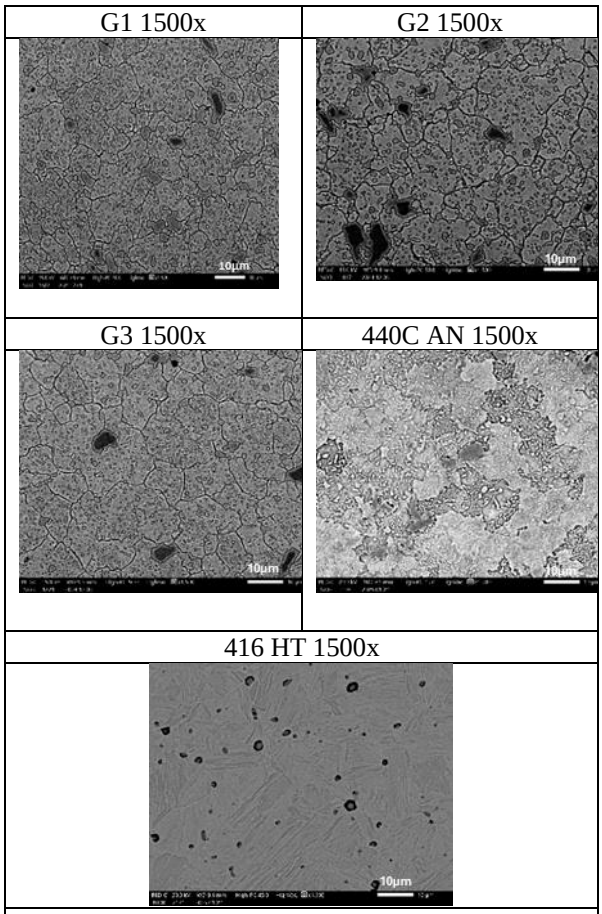


Figure 2 – SEM micrographs of etched samples by Viella's reagent

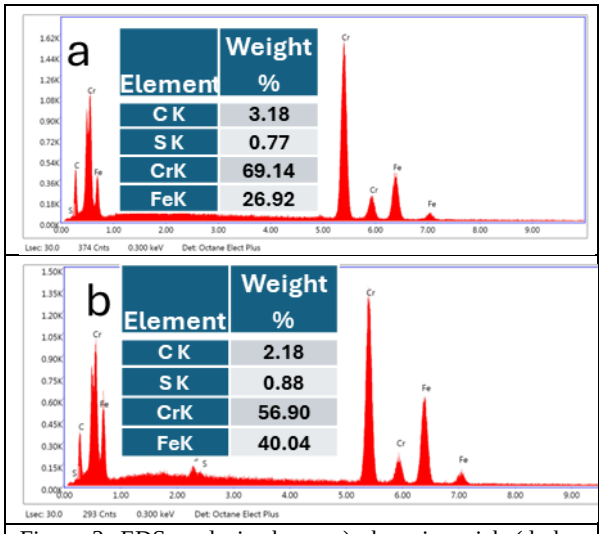


Figure 3: EDS analysis shows a) chromium-rich (darker precipitate) and b) chromium-lean regions within the carbide precipitates of the G1 group in 440C stainless steel.

Using the etched samples to see the grain structure the average size of the grains was calculated. The grain size analysis revealed after heat treatment of the 440C samples the grains increased in size, this is contradictory to what is expected as larger grains would result in a lower hardness but this is not what has been observed. The result of increased hardness after heat treatment is primarily due to the formation of precipitates during the heat treatment.

Table 3 – Average Grain Size

Sample	*416 HT*	*440C AN*	*G1*	*G2*	*G3*
Average grain area (µm²)	15.7	38.1	133.6	68.4	50.5
Average grain size (µm)	3.73	7.32	15.70	9.60	9.25

The average grain area data correlates with the grain size to show the trend in distribution of grains across the different samples. Grain size analysis shows 416 HT has the smallest average grain size (Table 3) amongst the samples, this is what supports its high hardness. 440C AN has a smaller average grain size in comparison to G1-G3 which have undergone heat treatment. What can be deduced from is that the grains have increased in size during the heat treatment process. During heat treatment, 440C steel is typically austenitised at high temperatures (1040°C). This process dissolves carbides and transforms the steel's structure into austenite. Higher austenitising temperatures can lead to grain growth (Figure 4) in the austenite phase. but as could be seen in the SEM analysis there are precipitates that have formed over the grains and on the grain boundaries.

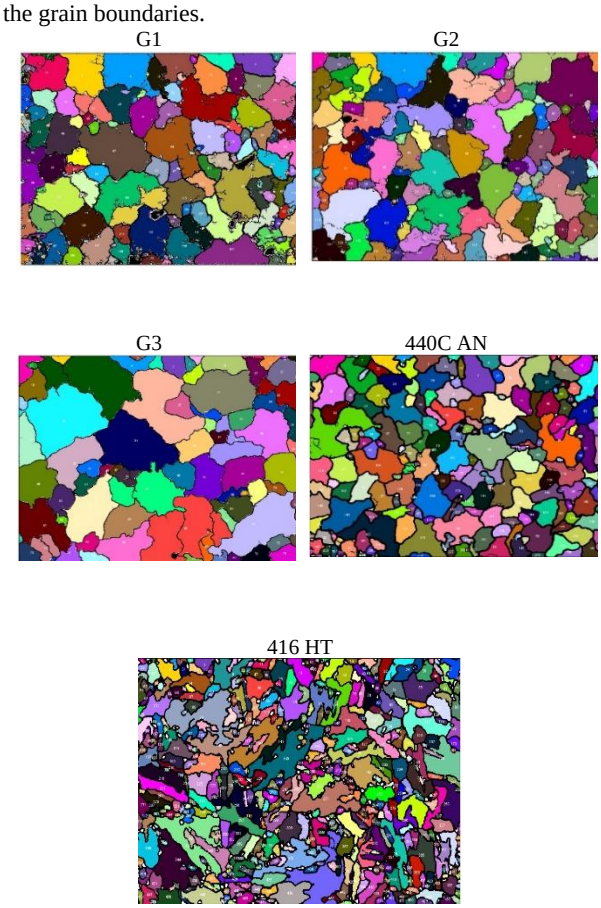


Figure 4 – Grain Size Analysis

The rapid cooling or quenching transforms the austenite into martensite, a hard and brittle phase. This process can also lead to the formation of various types of carbides, such as M7C3 and M23C6 [20], depending on the cooling rate and the presence of alloying elements like chromium and carbon. These precipitates play a critical role in the hardness of the material. Although the grains are bigger the Chromium Carbide precipitate in the material impede the further growth and movement of grains, pinning effect, resulting in a dramatic increase in overall hardness of the metal. However, at higher temperatures, the pinning effect is reduced, leading to larger grain sizes. The subsequent tempering after quenching helps to stabilise the microstructure, reduce residual stresses, and improve toughness.

EBSD is carried out on 440C AN and 416 HT (Figure 5) this is where electrons inside a SEM are shot onto a sample at a 70° which is known as Braggs angle, the electrons are backscattered creating different diffraction patterns called Kikuchi bands which are indexed against a database in order to identify the orientation of grains withing a material. From the EBSD scans carried out it shows grains within both materials are oriented in random directions this means there are no directional plains within the material where there would be weakness that could result in fracture.

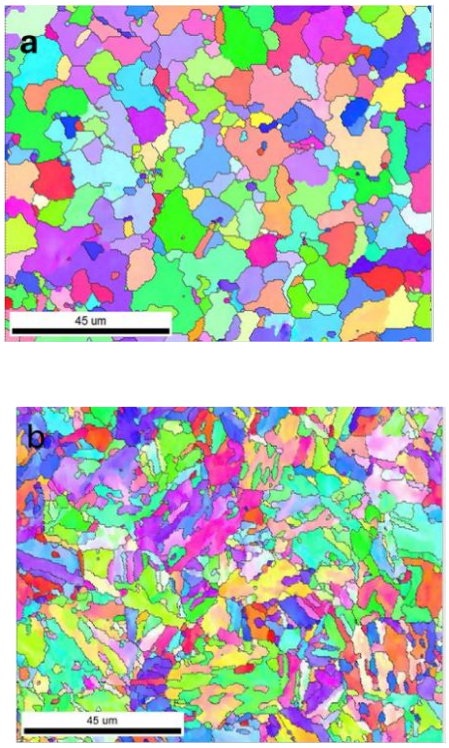


Figure 5 – EBSD of (a) 440C AN and (b) 416 HT

3.3 Corrosion Testing

The Open Circuit Potential (OCP) of annealed 440C stainless steel shows that by increasing the immersion time, the OCP shifts to a more negative potential. However, after a certain period (around 1000 seconds), the rate of change significantly

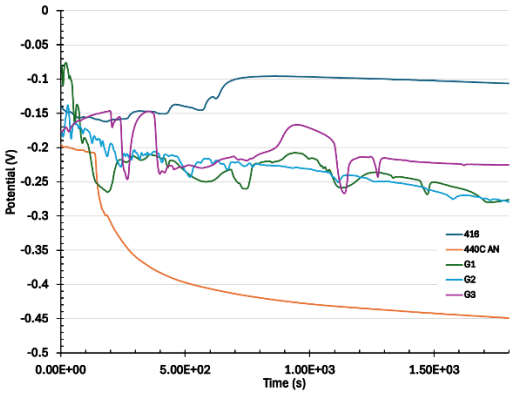


Figure 6 – OCP measurement of 416 and 440C at different heat treatment process

slows down and becomes relatively stable. In contrast, the OCP value for 416 stainless steel shifts to a more positive potential and reaches stability in a shorter time compared to the annealed 440C. This indicates that 416 stainless steel is potentially less active (in terms of corrosion) compared to the annealed 440C. This is because the OCP of 416 stainless steel is more positive (-0.1V) than that of the annealed 440C (-0.45V).

After heat treatment of the annealed 440C, it is observed that the OCP shifted to a more positive potential, which means that thermodynamically, the tendency of 440C to corrode after heat treatment is lower due to the shift to a more positive value. Among various types of heat treatments, heat treatment group 3 performed better than groups 1 and 2 because the final OCP reached stability in a shorter time and indicated a more positive potential compared to groups 1 and 2 (Figure 6). This means that thermodynamically, the corrosion tendency of the heat-treated sample in group 3 is lower than that of groups 1 and 2.

Potentiodynamic polarisation of the samples in 0.1 M NaCl solution indicates that 440C annealed has the lowest corrosion potential (-420 mV) and the highest corrosion current among all the 440C heat treated samples (Figure 7). This clearly shows that 440C without heat treatment has the lowest corrosion resistance in a corrosive environment. However, by performing heat treatment, the corrosion resistance is enhanced compared to the annealed 440C. Although different routes of heat treatment have varying effects on corrosion resistance, the best performance and enhanced corrosion resistance were obtained using the G3 route of heat treatment. In this situation, the corrosion potential shifted to -200 mV, indicating a shift to a more positive value (Table 4), and similarly, the corrosion current density reached a value of 345 nA/cm², which is significantly lower than the 5 µA/cm² of the annealed 440C. Although other routes of heat treatment such as G1 and G2 enhanced corrosion resistance, they are not as effective as the G3 route for enhancing corrosion resistance. Between the G1 and G2 routes of heat treatment, G1 provides slightly better corrosion resistance than G2 due to the lower corrosion current density and more positive corrosion potential.

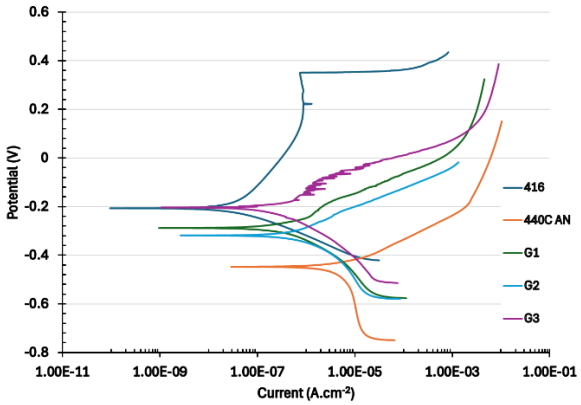


Figure 7 – PDP test of 416 and 440C in different heat treatment processes in 0.1M NaCl solution

Table 4 – PDP Testing Values

Sample	*Icorr (nA)*	*Ecorr (mV)*	*Corrosion Rate (mpy)*
440C AN	4920	-447	2.2460
G1	425	-288	0.1944
G2	809	-319	0.3696
G3	345	-204	0.1576
416 HT	42	-207	0.0192

3.4 Plastometry

Plastometery testing conducted on these five samples revealed the force required to reach an indent depth of 110µm is lower for both 440C AN and 416 HT in Comparison to G1-G3. The three heat treated 440C samples showed similar values in the region of 6kN of force required to reach the required indent depth (Figure 8). 440C AN required a third of that force to reach the same depth only needing 2kN to reach 110µm. 416 HT required 3.5kN of force for the indenter to reach the indent depth which shows the 440C AN is a softer material pre heat treatment in comparison to 416 HT.

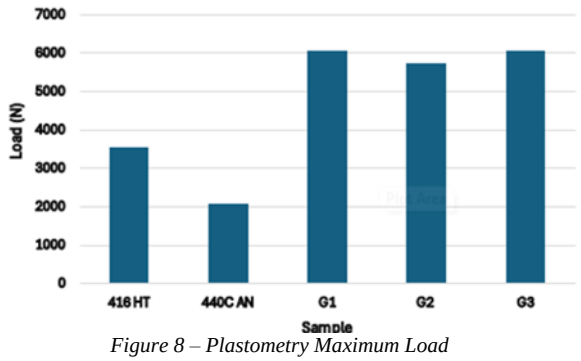


Figure 8 – Plastometry Maximum Load

Although the force required to reach the desired depth required more force for the heat treated 440C samples the residual indenter penetration is constant across all five samples. This reflects that the 440C heat treated samples have a greater resistance to deformation (Figure 9).

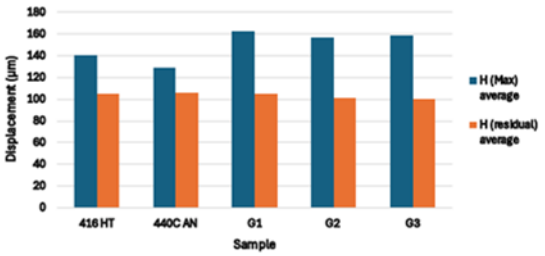


Figure 9 – Plastometry Maximum penetration and residual penatraiton

3.5 Pin on Disc

Testing shows all five samples undergoing friction wear testing over 30,000 while subjected to forces of 5N, 10N, 15N in separate tests. Under the load of 5N it is clear to see 440C AN has a higher coefficient of friction to the other 4 samples. When increasing the load to 10N all the samples are still consistent with the results from 5N besides one which is G3, the friction coefficient of G3 rises to almost the equivalent of 440C AN. Applying 15N to the friction test further extends this trend where the coefficient of G3 further increases to the point where it far exceeds that of the other samples (Figure 10). The initial results of 440C AN under 5N having a higher friction coefficient is due to the softness of the material in comparison to the others, this results in material removed from the surface of the steel causing more friction in the wear track. As 10N of force is applied the increase of the friction coefficient for G3 is led by its high martensite and carbide composition. Due to its hard phases and constituents any material eroded from the surface will greatly increase the friction as a third medium between the two testing surfaces this is further highlighted when 15N is applied. The reason this is not observed for G2 & G3 is due to the retained austenite phase that would be in the material due to its slower cooling stages. This retained austenite allows harder phases within the material to be compressed into the material during friction testing rather than break off within the wear track of the material. In steels containing chromium carbides, the wear behaviour is strongly influenced by the matrix phase: in a hard martensitic matrix, carbides tend to crack and detach under stress, leading to three-body abrasive wear and accelerated material loss; whereas in a softer austenitic matrix, carbides remain embedded due to the matrix's ductility, maintaining two-body wear and improving durability. Some studies show that while martensitic structures offer higher hardness, they risk brittle failure and carbide pull-out, whereas austenitic matrices can transform under strain to martensite, enhancing wear resistance without losing carbide cohesion[21, 22].

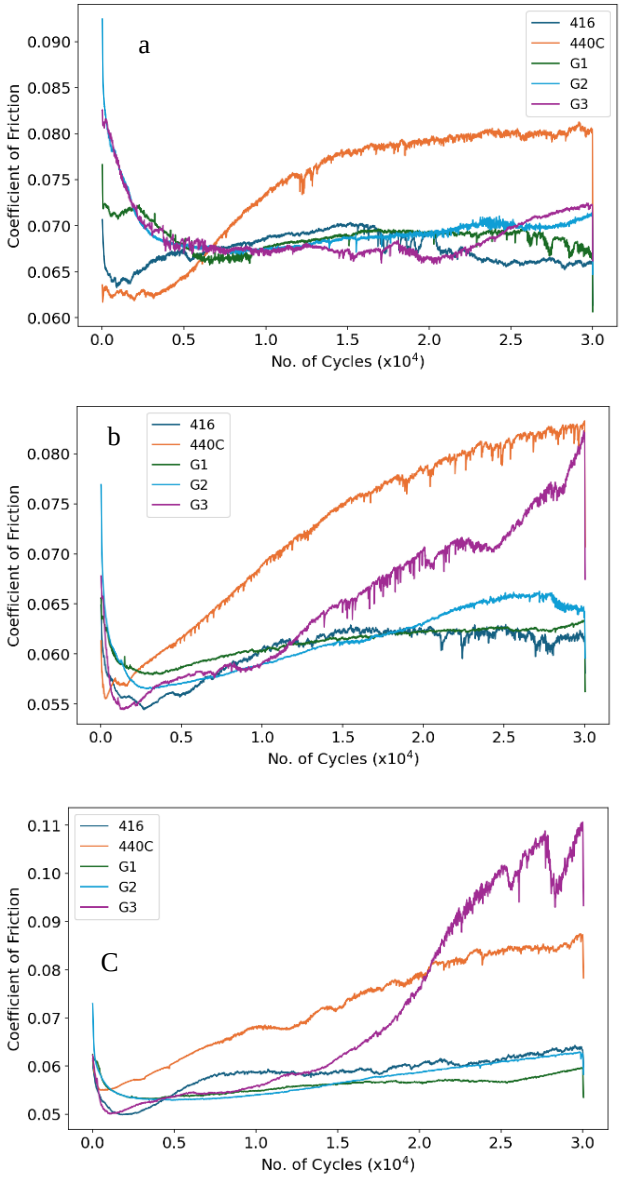


Figure 10 – Pin on disc testing with applied forces of 5N (a), 10N (b), 15N (c)

Material removal from the surface (Figure 11) of the samples due to friction varies across the loads applied to them. As expected, the higher the load the more material is worn away. G3 is observed to lose the least material under the testing with 440C AN and 416 HT showing to be the highest in material loss.

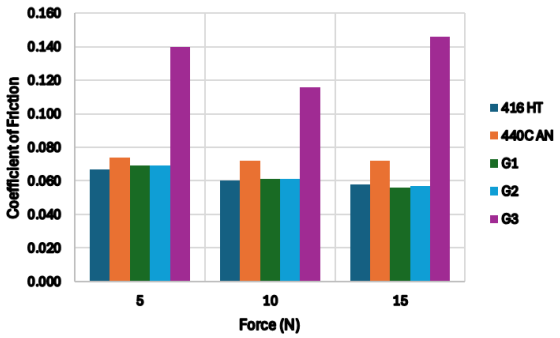


Figure 11 – Material loss

Material loss volume analysis carried out on the optical profiler in the Figure 12. This 3D surface map, generated using an optical profilometer, illustrates the topography of a wear track formed during tribological testing. The rendering highlights surface features such as grooves, pits, and material displacement caused by frictional contact. Depth variations across the track indicate localized wear severity, while the surrounding plateau regions represent unworn areas. The colour gradient corresponds to height differences, enabling quantitative analysis of wear depth, volume loss, and surface roughness. The surface roughness across the samples averaged at 3.5µ Sa with very little variation across each one.

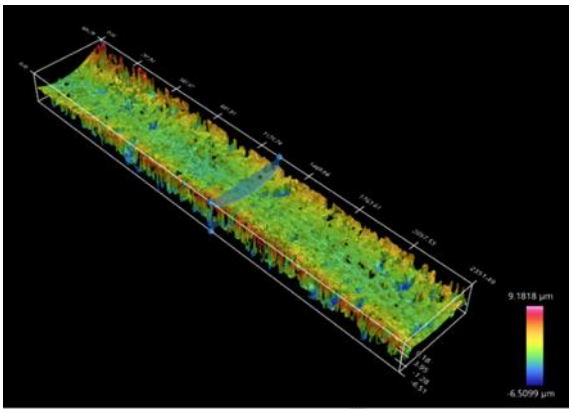


Figure 12 – 3D optical profilometer image showing surface topography of wear track with depth variations and material loss

4. CONCLUSION

This study evaluated the impact of different heat treatment routes on the mechanical and corrosion properties of 440C stainless steel, with comparative analysis against 416 stainless steel. Hardness testing showed that annealed 440C had a baseline hardness of approximately 19 HRC. After heat treatment, hardness increased significantly, ranging from 53 HRC to 59 HRC depending on the treatment route, representing a 140–165% improvement. In contrast, heat-treated 416 stainless steel reached a maximum hardness of ~43 HRC, confirming that 440C achieves substantially higher hardness under optimized conditions. This improvement is attributed to the formation of chromium carbides both at grain boundaries and within grains. Despite these mechanical gains,

corrosion resistance of 440C remains lower than that of 416, likely due to its higher carbon content and carbide precipitation. Among the heat treatment routes studied, the G3 route was the most effective, yielding the highest hardness (~59 HRC) and improving corrosion resistance by approximately 20% compared to other routes. Cryogenic cooling, which is part of the G3 heat treatment process, results in a smaller grain size compared to other heat treatment routes, namely G1 and G2. Additionally, the cryogenic cooling promotes the conversion of more austenite to martensite. This transformation leads to higher hardness in the alloy due to the increased formation of martensite compared to other heat treatment routes which has a significant effect on the friction behaviour of 440C. G3 exhibits a progressive increase in friction coefficient with rising load, surpassing all other samples at 15N due to its high martensite and carbide content. In contrast, samples with retained austenite, such as G2 and G1, show more stable wear behaviour due to softer austenite phase. Material loss analysis confirms G3's superior wear resistance, while 440C AN and 416 HT suffer the greatest volume loss under testing.

5. REFERENCES

[1] Baker I. Fifty Materials That Make the World. https://doi.org/10.1007/978-3-319-78766-4

[2] Bush R, Gill J, Teakell J. Heat Treatment Optimization and Fabrication of a 440C Stainless Steel Knife. JOM. 2016;68:3167-73. https://doi.org/10.1007/s11837-016-2117-5

[3] Rodríguez VM, Nadimpalli VK, Pedersen DB, Ruiz A. Nondestructive evaluation of tempering treatment in a spray-formed 440C martensitic stainless steel using thermoelectric power measurements. MRS Advances. 2025;10:108-14. https://doi.org/10.1557/s43580-024-01060-3

[4] Granta A. Stainless steel, martensitic, AISI 440C, tempered at 316°C. Granta 2024R2.

[5] Syarif J, H. Yousuf M, Sajuri Z, Baghdadi AH, Merabtene M, Omar MZ. Effect of Partial Solution Treatment Temperature on Microstructure and Tensile Properties of 440C Martensitic Stainless Steel. Metals2020. https://doi.org/10.3390/met10050694

[6] Rodríguez Herrejon V, Ruiz A, Bedolla-Jacuinde A, Nadimpalli VK. Comparative Analysis of Wear Properties of 440C Tool Steel Fabricated by Spray Forming and Conventional Casting. Journal of Materials Engineering and Performance. 2025. https://doi.org/10.1007/s11665-025-11860-9

[7] Idayan A, Gnanavelbabu A, Rajkumar K. Influence of Deep Cryogenic Treatment on the Mechanical Properties of AISI 440C Bearing Steel. Procedia Engineering. 2014;97:1683-91. https://doi.org/10.1016/j.proeng.2014.12.319

[8] Hetzner DW, Van Geertruyden W. Crystallography and metallography of carbides in high alloy steels. Materials Characterization. 2008;59:825-41. https://doi.org/10.1016/j.matchar.2007.07.005

[9] Yang J, Yu T, Wang C. Martensitic transformations in AISI 440C stainless steel. Materials Science and Engineering: A. 2006;438:276-80. https://doi.org/10.1016/j.msea.2006.02.098

[10] Syarif J, H. Yousuf M, Sajuri Z, Baghdadi AH, Merabtene M, Omar MZ. Effect of Partial Solution Treatment Temperature on Microstructure and Tensile Properties of 440C Martensitic Stainless Steel. Metals. 2020;10:694. https://doi.org/10.3390/met10050694

[11] Rodríguez VM, López-Morelos VH, Nadimpalli VK, Bue Pedersen D, Ruiz A, Somers MA. Effect of Heat Treatment Processes on the Microstructure and Mechanical Properties of Spray-Formed 440C Martensitic Stainless Steel. steel research international. 2023;94:2200749. https://doi.org/10.1002/srin.202200749

[12] Deng B, Yang D, Wang G, Hou Z, Yi H. Effects of Austenitizing Temperature on Tensile and Impact Properties of a Martensitic Stainless Steel Containing Metastable Retained Austenite. Materials. 2021;14:1000. https://doi.org/10.3390/ma14041000

[13] Campbell JE, Gaiser-Porter M, Gu W, Ooi S, Burley M, Dean J, et al. Indentation plastometry of very hard metals. Advanced Engineering Materials. 2022;24:2101398. https://doi.org/10.1002/adem.202101398

[14] Li X, Cui L, Li J, Chen Y, Han W, Shonkwiler S, et al. Automation of intercept method for grain size measurement: A topological skeleton approach. Materials & Design. 2022;224:111358. https://doi.org/10.1016/j.matdes.2022.111358

[15] Yang Z, Liu Z, Liang J, Yang Z, Sheng G. Elucidating the role of secondary cryogenic treatment on mechanical properties of a martensitic ultra-high strength stainless steel. Materials Characterization. 2021;178:111277. https://doi.org/10.1016/j.matchar.2021.111277

[16] Kara F, Ã‡iÃ§ek AÃi, Demir H. Effect of Deep Cryogenic Treatment on Microstructure, Mechanical Properties, and Residual Stress of AISI 52100 Bearing Steel. Engineered Science. 2023;26:960. https://doi.org/10.30919/es960

[17] Brunatto SF, Cardoso RP, Santos LL. Behavior of Retained Austenite and Carbide Phases in AISI 440C Martensitic Stainless Steel under Cavitation. Eng2024. p. 1980-94. https://doi.org/10.3390/eng5030105

[18] Krishna SC, Tharian KT, Chakravarthi KVA, Jha AK, Pant B. Heat Treatment and Thermo-Mechanical Treatment to Modify Carbide Banding in AISI 440C Steel: A Case Study. Metallography, Microstructure, and Analysis. 2016;5:108-15. https://doi.org/10.1007/s13632-016-0266-0

[19] Liu B-b, Zhang H, Xu X-y, Tian Q-r, Fu J-x. Analysis of Cracking Causes of AISI 416 Martensitic Stainless Steel During Hot Rolling. Transactions of the Indian Institute of Metals. 2023;76:2643-50. https://doi.org/10.1007/s12666-023-02942-0

[20] Krishna SC, Tharian KT, Chakravarthi K, Jha AK, Pant B. Heat treatment and thermo-mechanical treatment to modify carbide banding in AISI 440C steel: a case study.

Metallography, Microstructure, and Analysis. 2016;5:108-15. https://doi.org/10.1007/s13632-016-0266-0

[21] Iakovakis E, Avcu E, Roy MJ, Gee M, Matthews A. Wear resistance of an additively manufactured high-carbon martensitic stainless steel. Scientific Reports. 2022;12:12554. https://doi.org/10.1038/s41598-022-15621-9

[22] Todaka T, Shimizu K, Kusumoto K, Purba RH, Gaqi Y. Effect of Carbon Content on Three-body Abrasive Wear Characteristics of 28Cr-3Ni Cast Alloys. ISIJ International. 2021;61:2274-83. https://doi.org/10.2355/isijinternational.ISIJINT-2021-099